
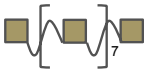




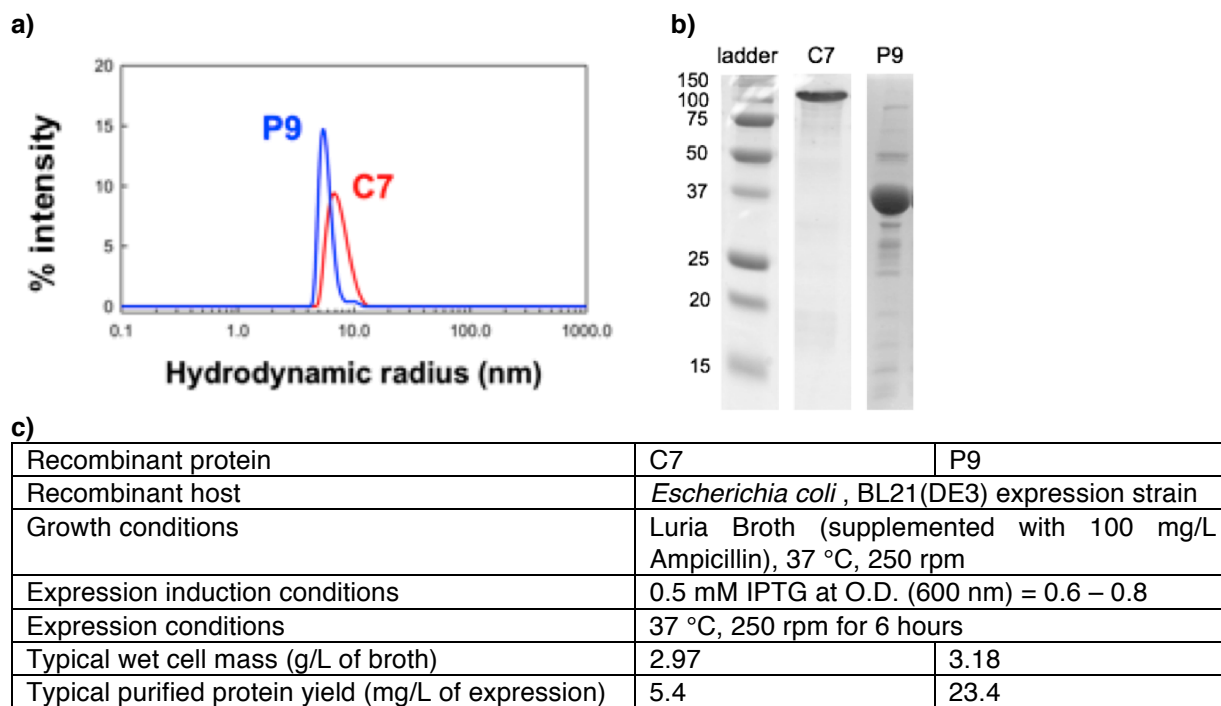


## Supplementary Information

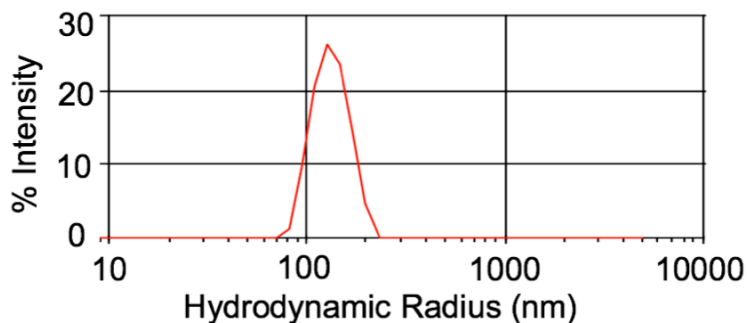
### Supplementary Figures

MITCH Components	Schematic	Amino Acid Sequence
C7		MGSSHHHHHHSSGLVPRGSSSGHIDDDDKVDGT [RLPAGWEQRMDVKGRPYFVDHVTKSTTWEDPRPE] GTLDEL [AGAGAGPEG] <sub>2</sub> RGDSAGPEG [AGAGAGPEG] <sub>2</sub> ELLDGT ( [RLPAGWEQRMDVKGRPYFVDHVTKSTTWEDPRPE] GTLDEL [AGAGAGPEG] <sub>2</sub> [RGDSAGPEG] [AGAGAGPEG] <sub>2</sub> ELLDGT ) <sub>5</sub> [RLPAGWEQRMDVKGRPYFVDHVTKSTTWEDPRPE] GTLE
P9		MGSSHHHHHHSSGLVPRGSSSGHIDDDDKVDGT [EYPPYPPPPYPSG] GTLDEL [AGAGAGPEG] <sub>2</sub> ELLDGT ( [EYPPYPPPPYPSG] GTLDEL [AGAGAGPEG] <sub>2</sub> ELLDGT ) <sub>7</sub> [EYPPYPPPPYPSG] GTLE
Peptide Modules	Schematic	Amino Acid Sequence
CC43 WW domain		RLPAGWEQRMDVKGRPYFVDHVTKSTTWEDPRPE
Proline-rich peptide		EYPPYPPPPYPSG
Hydrophilic spacer		[AGAGAGPEG] <sub>2</sub>
Cell-binding site		RGDSAGPEG

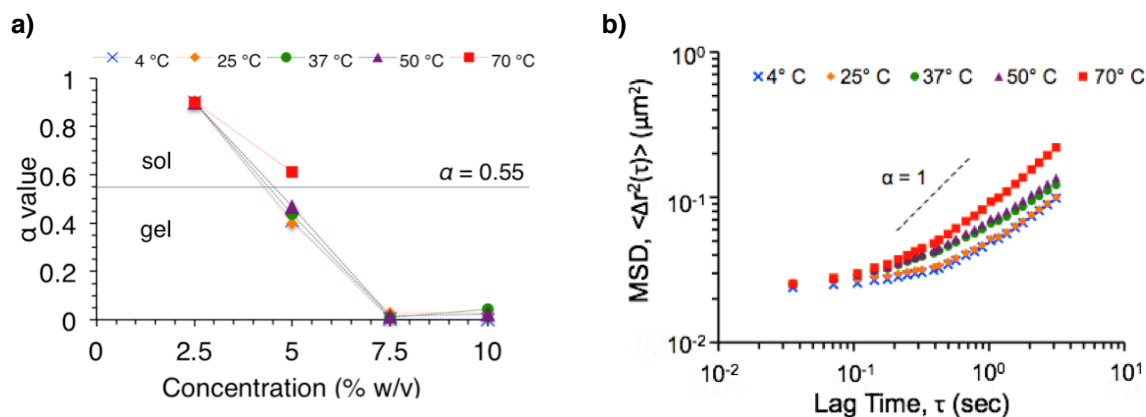
**Figure S1.** Modular design of MITCH, showing the amino acid sequences of C7 and P9 block copolymers and the constituent peptide modules.



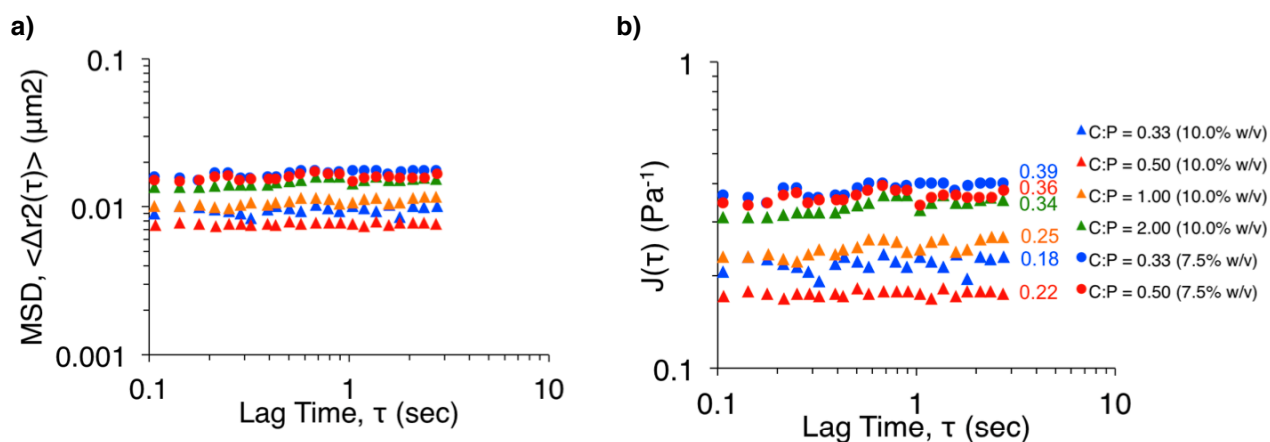
**Figure S2.** Molecular size and composition of purified proteins. (a) Dynamic light scattering histograms showing the percentage of scattering mass versus hydrodynamic radius ( $R_H$ ). C7 and P9 have narrow radius distributions, averaging at 6.2 nm and 5.3 nm respectively. (b) SDS polyacrylamide gel electropherograms of C7 and P9. The molecular weights of C7 and P9 are 60.89 kg/mol and 37.61 kg/mol, respectively. Due to the high occurrence of acidic and hydrophilic amino acids, the spacers in C7 bind the anionic surfactant SDS weakly, resulting in a reduced effective charge and low electrophoretic mobility. Hence, the molecular weight of C7 appears larger than the actual value. Additional characterization by mass spectrometry and amino acid analysis have been reported elsewhere,<sup>1</sup> confirming the correct molecular weight and composition of C7 and P9. (c) Recombinant expression conditions of C7 and P9, and yields of purified protein.



**Figure S3.** Dynamic light scattering histograms showing the size distribution of fluorescent polystyrene tracers at 37 °C. Particles were diluted in buffer TN (100 mM TrisHCl and 100 mM NaCl, pH 8.0) to achieve the same salt condition and particle volume fraction as those used in microrheology. The single-peak distribution indicates single particle suspensions (actual diameter = 0.21  $\mu\text{m}$ , as reported by Molecular Probes), confirming the absence of particle aggregation.



**Figure S4.** (a) Logarithmic slope  $\alpha$  of micrheological mean-squared displacement ( $MSD$ ) versus lag time graphs, used to define the criteria for gelation. Samples whose  $\alpha$  values lie above and below 0 are classified as sol and gel, respectively. (b)  $MSD$  versus lag time for C7:P9 gels prepared at 5.0% w/v. Increase in temperature caused the  $\alpha$  value to increase, indicating a transition toward liquid-like behavior.



**Figure S5.** (a) Microrheological mean-squared-displacement ( $MSD$ ) versus lag time for C7:P9 gels prepared at various concentrations and C:P ratios. Increasing the concentration from 7.5% to 10.0% w/v resulted in a decrease in  $MSD$ . At a given concentration, minimum  $MSD$  values corresponding to highest storage moduli ( $G'$ ) were obtained at a C:P ratio of 0.50. (b) Creep compliance  $J(t)$  of C7:P9 gels, calculated from the  $MSD$  data according to the relation  $J(\tau) = (3\pi r/2k_B T) \langle \Delta r^2(\tau) \rangle$  (ref 2). Creep compliance remains approximately constant with lag time, indicating the formation of stable hydrogel network. Values of steady state creep compliance,  $J_e^0$ , computed from the average of  $J(\tau)$ , are stated next to the corresponding data sets.

## References

- (1) Wong Po Foo, C. T.; Lee, J. S.; Mulyasmita, W.; Parisi-Amon, A.; Heilshorn, S. C. Proc Natl Acad Sci U S A 2009, 106, 22067.
- (2) Wirtz, D. Annu Rev Biophys 2009, 38, 301.